

Collaborative Semantic Aggregation and Calibration for Separated Domain Generalization

Junkun Yuan, Xu Ma, Defang Chen, Kun Kuang, Fei Wu, Lanfen Lin

Abstract

Domain generalization (DG) aims to learn from multiple known source domains a model that can generalize well to unknown target domains. The existing DG methods usually rely on shared multi-source data fusion for generalizable model training. However, tremendous data is distributed across lots of places nowadays that can not be shared due to privacy policies, especially in some crucial areas like finance and medical care. A dilemma is thus raised between real-world data privacy protection and simultaneous multi-source semantic learning with the shared data. In this paper, we investigate a separated domain generalization task with separated source datasets that can only be used locally, which is vital for real-world privacy protection. We propose a novel solution called Collaborative Semantic Aggregation and Calibration (CSAC) to enable this challenging task. To fully absorb multi-source semantic information while avoiding unsafe data fusion, we first conduct data-free semantic aggregation by fusing the models trained on the separated domains layer-by-layer. To address semantic dislocation caused by domain shift, we further design cross-layer semantic calibration with an attention mechanism to align each semantic level and enhance domain invariance. We unify multi-source semantic learning and alignment in a collaborative way by repeating the semantic aggregation and calibration alternately, keeping each dataset localized, and privacy is thus carefully protected. Extensive experiments show the significant performance of our method in addressing this challenging task, which is even comparable to the previous DG methods with shared data.

Introduction

Recently, deep learning has made revolutionary advances to visual recognition (He et al. 2016), under the i.i.d. assumption that training and test data are sampled from the same distribution. Since the adopted datasets could be very distinct in real applications, the deep models learned from one training (source) dataset may cause severe performance degradation on another test (target) dataset. To address this *dataset/domain shift* (Quionero-Candela et al. 2009) problem, *domain generalization* (DG) (Blanchard, Lee, and Scott 2011) is introduced for training a generalizable model to unknown out-of-distribution target domains by learning from multiple semantically relevant source datasets/domains.

yuanjk@zju.edu.cn

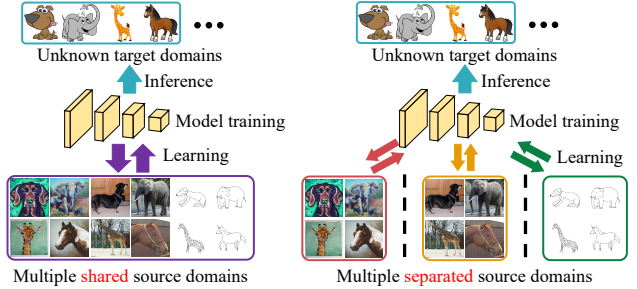


Figure 1: Comparison of the generic domain generalization task (**left**) and the investigated *separated domain generalization* task (**right**). The latter is more challenging yet significant for data privacy protection in real-world applications.

Numerous DG methods (Dou et al. 2019; Carlucci et al. 2019; Zhao et al. 2020) have been proposed recently. They popularize a variety of favorable strategies for generalizable model training by (indirectly) using the fusion of “*shared*” multi-source data. For example, some alignment-based methods (Li et al. 2018b,c; Zhao et al. 2020) match multi-source data distributions in latent space for learning domain-invariant feature representations; and some meta-learning-based strategies (Dou et al. 2019; Li et al. 2019a,b) utilize meta-train and meta-test datasets built by sampling from multi-source data for training a stable model to unknown domains. However, these previous methods may seriously violate data privacy policies, as tremendous data is stored locally in separated places nowadays, which may contain private information, e.g., patient data from the hospitals and video recording from the surveillance cameras. A dilemma is then encountered between real-world data privacy protection and simultaneous multi-source semantic learning with shared data for generalization improvement.

In this paper, we investigate *separated domain generalization* (see Figure 1), where the source datasets are separated and can only be used locally. It is vital for real-world data privacy protection, and more challenging as: (1) the separated source datasets are private and can not be directly fused, hence the simultaneous learning of the multi-source semantic information is greatly hindered, making domain invariance identification tricky; (2) the heterogeneous

source datasets with distinct data distributions may constitute enormous obstacles for generalizable model training as the model can only access one local data each time, while the accessed data may contain particularly unusual bias, making the trained model exhibit a negative generalization gain.

We propose a novel solution with Collaborative Semantic Aggregation and Calibration (CSAC) to enable separated domain generalization. We first hypothesize that the deep models extract semantic information from low-level to high-level, and the model parameters in each layer are related to the corresponding semantic level as well as the training data distribution (proof-of-concept experiments are provided in Appendix to verify it). In light of this, to fully absorb multi-source semantic information while avoiding unsafe data fusion, a data-free semantic aggregation strategy is devised to fuse the models trained on the separated domains layer-by-layer. Then a semantic dislocation problem has arisen: Due to domain shift, the same level of semantic information from different domains could be distributed across model layers during the aggregation. Therefore, we further design cross-layer semantic calibration with an attention mechanism for precise semantic level alignment and domain-invariance enhancement. We unify the multi-source semantic learning and alignment in a collaborative way by repeating the semantic aggregation and calibration alternately, keeping each source dataset localized, and privacy is thus carefully protected.

Our contributions are: (1) By pointing out the dilemma of the existing DG methods between generalizable model training and data privacy protection, we investigate separated domain generalization, which is significant for real-world data privacy protection; (2) To tackle this challenging problem, we propose privacy-preserving Collaborative Semantic Aggregation and Calibration (CSAC) to unify the multi-source semantic learning and alignment in a collaborative way by repeating data-free semantic aggregation and cross-layer semantic calibration alternately; (3) Extensive experiments show the significant performance of our method in addressing this challenging problem, which is even comparable to the previous DG methods with shared source data.

Related Work

Domain generalization. Domain generalization (DG) (Blanchard, Lee, and Scott 2011) aims to train a generalizable model by utilizing multiple source datasets. A direct idea for DG is to align multi-source data distributions in latent space for learning invariant semantic feature representation (Li et al. 2018b; Qiao, Zhao, and Peng 2020; Li et al. 2018c,d; Matsuura and Harada 2020; Zhao et al. 2020; Li et al. 2020a; Piratla, Netrapalli, and Sarawagi 2020), which is also widely adopted in domain adaptation (Ganin et al. 2016; Long et al. 2015, 2017). For example, Li et al. extract domain-invariant representations of multi-source joint distributions through a conditional invariant adversarial network. Another set of strategies (Balaji, Sankaranarayanan, and Chellappa 2018; Li et al. 2018a; Dou et al. 2019; Li et al. 2019a,b) are based on meta-learning, they employ an episodic training paradigm that trains the model and improves its out-of-distribution generalization ability on meta-train and meta-test datasets, respectively, which are built

from the shared multi-source data. For instance, Dou et al. present a model-agnostic meta-learning training paradigm with two complementary losses to consider both global knowledge and local cohesion. Data augmentation (Shankar et al. 2018; Volpi et al. 2018; Carlucci et al. 2019; Zhou et al. 2020a; Wang et al. 2020; Zhou et al. 2020b, 2021) for DG is also popular by training the model on generated novel domains for generalization improvement. JiGen (Carlucci et al. 2019) is a representative work that trains the model on the generated data for solving a jigsaw puzzle. Some other works (Chattpadhyay, Balaji, and Hoffman 2020; Huang et al. 2020; Seo et al. 2020) optimize the regularization terms of the data or networks to gain generalization performance.

However, most of these methods are in thrall to shared multi-source data for generalizable model training, concerns about data privacy are thus raised, as tremendous private data is distributed across separated places in real scenarios.

Federated learning. Federated learning (FL) (McMahan et al. 2017; Yang et al. 2019) is an active research field nowadays (Lin et al. 2020; Yoon et al. 2021; Ghosh et al. 2020). FL makes local clients jointly train a model with a central server and keeps data decentralized for data privacy protection. Take a representative paradigm FedAvg (McMahan et al. 2017) as an example. In each communication round, a subset of the clients is chosen to receive the parameters of a global model from the server and train it on their local data. The trained models are then transmitted back to the server for updating the global model with data size based weights.

The investigated separated domain generalization task is closely related to FL as the data is decentralized, but the former is much more challenging: FL mainly focuses on guaranteeing model convergence when training on non-i.i.d. data (Yang et al. 2019), and improving model performance on the “known” clients; In contrast, our goal is to capture domain invariance from separated domains and construct a generalizable model for “unknown” out-of-distribution domains.

Distributed domain adaptation and generalization. Source-free domain adaptation (Kundu et al. 2020; Li et al. 2020b) improves performance on the target domain by only using a source pretrained model. FL-based domain adaptation (Peng et al. 2020) adapts models from distributed source domains to target domains. The above domain adaptation problem needs to collect data and perform model tuning for each new target domain, which is expensive or even infeasible in real applications. FedDG (Liu et al. 2021) is proposed to learn a generalizable model in FL setting with frequency space interpolation for medical image segmentation. However, it builds an amplitude spectrum distribution bank from the source data and shares it to all the clients, which: (1) is time-consuming for building the bank and expensive for data storage; (2) needs high communication costs to transmit the bank to all the clients; (3) shares the amplitude spectrum of the source data to all the clients that may increase the risks of data privacy leakage. In contrast, we do not have extra time-consuming procedures like building such a distribution bank. More importantly, we do not share any data (or parts of its information) during model training for efficient communication and adequate privacy protection, but learn a model with higher out-of-distribution generalization performance.

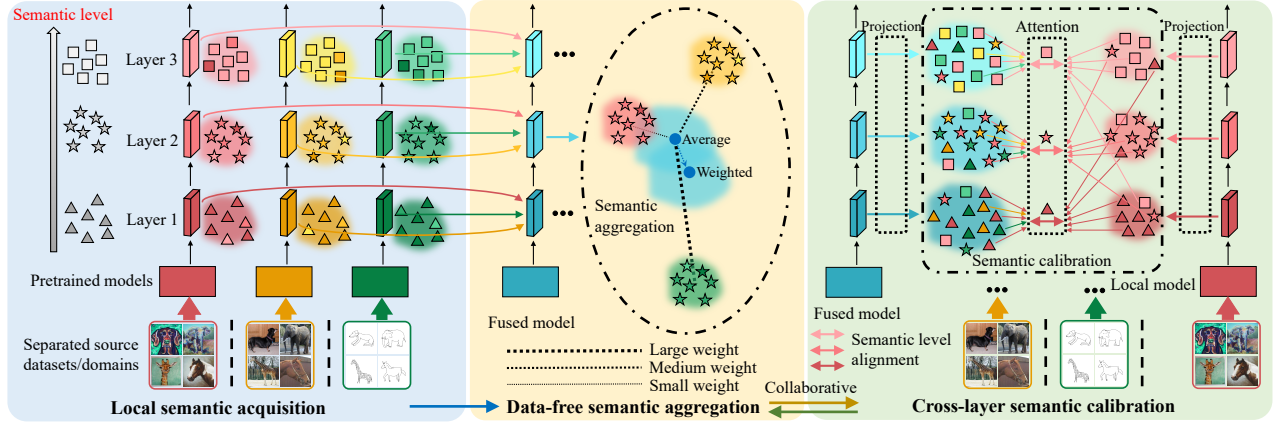


Figure 2: Overview of the proposed Collaborative Semantic Aggregation and Calibration (CSAC). **Left:** Each domain is assigned a model for distribution learning, which extracts semantic information from low-level to high-level, i.e., ▲, ★, and ■; **Middle:** The trained models are fused layer-by-layer for multi-source semantic gathering; **Right:** Cross-layer pairs between the fused model and each local model are matched with attention, for semantic level alignment and domain invariance enhancement.

Method

We begin with the problem definition of the investigated separated domain generalization and its challenges for generalizable model training. We then introduce our novel solution (see Figure 2) for addressing this challenging task in detail.

Separated Domain Generalization

In separated domain generalization, we have source datasets $\{\mathcal{D}^1, \dots, \mathcal{D}^H\}$ from H separated domains. There are N^h samples in each dataset \mathcal{D}^h , i.e., $\mathcal{D}^h = \{(x_i^h, y_i^h)\}_{i=1}^{N^h}$, defined on image and label spaces $\mathcal{X} \times \mathcal{Y}$. The goal is to utilize the separated source datasets for training a generalizable model, which can perform well on unknown target domains. Note that we consider heterogeneous source data with the same data space but different distributions, and adopt hierarchical deep models with the same architecture for learning.

The challenges of this task are: (1) The source datasets are separated and can only be utilized locally, which greatly hinders the simultaneous learning of the multi-source semantic information, leading to invalid domain invariance identification; (2) The heterogeneous source datasets with distinct data distributions constitute enormous obstacles for generalizable model training, as the model can only access one local data each time. That is, if the accessed data contains particularly unusual domain-specific bias, the trained model may even exhibit a negative generalization gain.

The core idea of our **solution** CSAC (Figure 2) is to fully absorb multi-source information and precisely align semantic levels, which contains three main processes: (1) *Local semantic acquisition* for data distribution information learning; (2) *Data-free semantic aggregation* for multi-source semantic information gathering; and (3) *Cross-layer semantic calibration* for semantic level alignment and domain-invariance enhancement. After obtaining the distribution information in process (1), the latter two processes are repeated alternately, unifying the multi-source semantic learning and alignment in a collaborative way for generalizable model training. It is worth mentioning that we *only transmit*

models between the separated domains, and neither data nor its information is shared for adequate privacy protection.

Local Semantic Acquisition

Before learning and aligning the multi-source semantic information, we need to fully absorb the data distribution information of the source datasets. To avoid unsafe data fusion, we assign one model on each of the separated domains to impose data distribution learning. Given H separated source datasets, y^h with C categories is the ground-truth label of the image x^h in dataset \mathcal{D}^h , where $h \in \{1, \dots, H\}$. Let $\{G^h\}_{h=1}^H$ be the trained models, each model G^h can be optimized on the source data \mathcal{D}^h with the cross-entropy loss

$$\mathcal{L}_{CE} = -\mathbb{E}_{(x^h, y^h)} [\sum_{c=1}^C \mathbb{1}(y^h = c) \log G^h(x^h)], \quad (1)$$

where $\mathbb{1}(\cdot)$ is an indicator function values 1 for the correct condition, and 0 for the rest. To facilitate the following semantic aggregation and calibration, we further introduce label smoothing for encouraging data to distribute in tight evenly separated clusters (Müller, Kornblith, and Hinton 2019; Liang, Hu, and Feng 2020). The updated loss is

$$\mathcal{L}_{CE}^{LS} = -\mathbb{E}_{(x^h, y^h)} [\sum_{c=1}^C p_c^h \log G^h(x^h)], \quad (2)$$

where $p_c^h = (1-\alpha) \mathbb{1}(y^h = c) + \alpha/K$ is the smoothed label, and α is a smoothing hyper-parameter empirically set to 0.1.

Data-Free Semantic Aggregation

After acquiring multi-source data information, we devise data-free semantic aggregation with the trained models $\{G^h\}_{h=1}^H$. Inspired by recent researches (Wang et al. 2018; Zhang et al. 2019b) on the interpretability of deep neural networks, we hypothesize that the deep models extract semantic information from low-level to high-level, and the model parameters in each layer are related to the corresponding semantic level as well as the training data distribution (we will

discuss it in detail with proof-of-concept experiments in Appendix). As each model G^h trained on the local data \mathcal{D}^h , it extracts hierarchical semantic information from the data distributions. Let G_l^h be the l -th layer of the model G^h , we have an average model parameter distribution of the l -th layer

$$G_l^{AVG} = \frac{1}{H} \sum_{h=1}^H G_l^h. \quad (3)$$

We then find that if a source data have a distribution far from the others, the corresponding model would be considered less as it is also far from the average distribution G_l^{AVG} . To fairly absorb the information of the source datasets for precise semantic calibration, we assign weight to each model based on its semantic divergence to the average distribution:

$$M_l = \sum_{h=1}^H \frac{\text{dist}(G_l^h, G_l^{AVG})}{\sum_{h=1}^H \text{dist}(G_l^h, G_l^{AVG})} G_l^h, \quad (4)$$

where M_l is the l -th layer of the fused model M , and $\text{dist}(\cdot, \cdot)$ is distance metric and empirically used as L_2 distance. Models with distinctive parameters, or training data distributions, will be paid more attention to by being given a large weight. As the trained models are fused layer-by-layer, different levels of semantic information from the separated source domains are aggregated indirectly for domain invariance learning in the semantic calibration process.

Cross-Layer Semantic Calibration

Due to the distinct data distributions of the source datasets, i.e., domain shift, the same level of semantic information from different domains could be distributed across the layers of the fused model M during the aggregation process, which we call the *semantic dislocation* problem. To calibrate each level of semantic information for improving model generalization, we align each cross-layer semantic feature pair between the fused model M and a local model L^h trained on each local source domain like G^h . Take Figure 2 (right) as an example. The second layer of the fused model mainly contains the second level of semantic information from different domains, i.e., \star in different colors. We match it with each layer of a local model to align the second semantic level, i.e., match \star in different layers of the local model, where each cross-layer pair is weighted by their semantic similarities. Since the hierarchical semantic features may have different size, we first project them to the same size (we use the size of the smallest semantic features in the experiments):

$$\begin{aligned} M_l(x^h)' &= \text{Proj}(M_l(x^h)), \\ L_m^h(x^h)' &= \text{Proj}(L_m^h(x^h)), \end{aligned} \quad (5)$$

where $\text{Proj}(\cdot)$ is the projection function with one convolution layer (see Appendix for details). We then align each cross-layer semantic feature pair (l, m) after projection by

$$\mathcal{L}_{AL}^h = \sum_{l \in \mathcal{R}} \sum_{m \in \mathcal{R}} \alpha_{l,m} D(M_l(x^h)', L_m^h(x^h)'), \quad (6)$$

where $D(\cdot, \cdot)$ is used to measure the distribution discrepancy, which is minimized to perform semantic feature

alignment. We adopt Maximum Mean Discrepancy (MMD) (Gretton et al. 2012) for it by following (Long et al. 2016; Venkateswara et al. 2017). The set of layers \mathcal{R} for alignment is given in experiments. A dynamic weight $\alpha_{l,m}$ for the layer pair (l, m) is learned by an attention mechanism.

Attention mechanism. To encourage the cross-layer pairs with greater semantic similarity to be matched for precise semantic level alignment and domain invariance enhancement, while weakening the pairs with less similarity for avoiding further semantic dislocation, we then introduce a semantic similarity-based attention mechanism. Attention (Bahdanau, Cho, and Bengio 2015) is a widely adopted technique (Wang et al. 2017; Zhang et al. 2019a; Fu et al. 2019) for deciding which parts of the input features should be paid more attention to. Here, we consider the semantic inter-dependencies in both *position* and *channel* dimensions. Let c, g , and w be the channel, height, and width of the semantic features after projection, respectively. We first reshape $M_l(x)'$ $\in \mathcal{R}^{c \times g \times w}$ and $L_m^h(x)'$ $\in \mathcal{R}^{c \times g \times w}$ to $A_l \in \mathcal{R}^{c \times d}$ and $B_m \in \mathcal{R}^{c \times d}$, respectively, where $d = g \times w$ is the number of pixels in an image. Then, we have a position-wise weight

$$\alpha_{l,m}^p = \frac{\exp(\text{avg}(A_l^\top B_m))}{\sum_{m \in \mathcal{R}} \exp(\text{avg}(A_l^\top B_m))}, \quad (7)$$

where $A_l^\top B_m$ is the position-wise attention map, measuring the response of A_l to B_m , i.e., the l -th layer of the fused model M_l to the m -th layer of the local model L_m^h . The operator $\text{Avg}(\cdot)$ averages the attention map to a real number, and the weight $\alpha_{l,m}^p$ is the normalization of the average position-wise semantic similarity. Similarly, we have

$$\alpha_{l,m}^c = \frac{\exp(\text{avg}(A_l B_m^\top))}{\sum_{m \in \mathcal{R}} \exp(\text{avg}(A_l B_m^\top))}. \quad (8)$$

$\alpha_{l,m}^c$ measures the channel-wise semantic similarities. We average them to get the final weight for the pair (l, m) :

$$\alpha_{l,m} = \frac{1}{2} (\alpha_{l,m}^p + \alpha_{l,m}^c). \quad (9)$$

$\alpha_{l,m}$ characterizes the inter-dependencies between the fused model G_l and local model L_m^h in both position and channel dimensions, weighting cross-layer pairs for precise semantic level alignment and domain invariance enhancement.

Since the semantic information from each domain is aggregated with other domains, the fused model may suffer from the *catastrophic forgetting* problem (McCloskey and Cohen 1989; Goodfellow et al. 2013), i.e., the data knowledge in the model is gradually forgotten when incrementally updating models with other data knowledge. We thus employ cross-entropy loss for retraining M on each data \mathcal{D}^h ,

$$\mathcal{L}_{CE}^h = -\mathbb{E}_{(x^h, y^h)} [\sum_{c=1}^C \mathbb{1}(y^h = c) \log M(x^h)]. \quad (10)$$

Then we have the calibration loss on each source data \mathcal{D}^h :

$$\mathcal{L}_{CB}^h = \lambda \mathcal{L}_{AL}^h + \mathcal{L}_{CE}^h, \quad (11)$$

Table 1: Classification accuracy (%) on rotated MNIST dataset. “Sep.”: whether using separated source datasets.

Methods	Sep.	M0	M15	M30	M45	M60	M75	Average
DeepAll*	✗	86.73 \pm 0.45	98.27 \pm 0.40	98.63 \pm 0.15	97.50 \pm 0.89	97.47 \pm 0.25	87.20 \pm 0.95	94.30 \pm 0.29
CrossGrad	✗	86.03	98.92	98.60	98.39	98.68	88.94	94.93
MetaReg	✗	85.70	98.87	98.32	98.58	98.93	89.44	94.97
FeaCri	✗	87.04	99.53	99.41	99.52	99.23	91.52	96.04
DGER	✗	90.09	99.24	99.27	99.31	99.45	90.81	96.36
FedAvg*	✓	82.60 \pm 0.44	98.56 \pm 0.27	98.97 \pm 0.29	93.66 \pm 0.03	95.78 \pm 0.27	86.30 \pm 0.10	92.65 \pm 0.08
FedDG*	✓	73.07 \pm 0.67	94.37 \pm 1.03	95.60 \pm 0.19	89.43 \pm 0.38	94.61 \pm 0.39	84.50 \pm 0.10	88.60 \pm 0.30
CSAC	✓	84.57 \pm 0.31	98.87 \pm 0.23	98.63 \pm 0.15	95.06 \pm 0.48	96.57 \pm 0.40	90.73 \pm 0.25	94.07 \pm 0.02

Table 2: Classification accuracy (%) on VLCS dataset. “Sep.”: whether using separated source datasets.

Methods	Sep.	Pascal	LabelMe	Caltech	Sun	Average
AlexNet						
DeepAll*	✗	71.67 \pm 0.26	59.64 \pm 0.81	97.48 \pm 0.14	67.58 \pm 0.68	74.09 \pm 0.17
Epi-FCR	✗	67.1	64.3	94.1	65.9	72.9
JiGen	✗	70.62	60.90	96.93	64.30	73.19
MASF	✗	69.14	64.90	94.78	67.64	74.11
DGER	✗	73.24	58.26	96.92	69.10	74.38
EISNet	✗	69.83	63.49	97.33	68.02	74.67
FedAvg*	✓	67.92 \pm 0.26	60.23 \pm 0.81	96.85 \pm 0.26	66.88 \pm 0.22	72.97 \pm 0.16
FedDG*	✓	67.27 \pm 0.07	58.48 \pm 0.04	96.83 \pm 0.47	68.20 \pm 0.12	72.69 \pm 0.16
CSAC	✓	69.52 \pm 0.14	60.05 \pm 0.05	97.48 \pm 0.30	69.22 \pm 0.15	74.07 \pm 0.01
ResNet-18						
DeepAll*	✗	71.40 \pm 0.32	59.77 \pm 0.95	97.54 \pm 0.54	69.01 \pm 0.25	74.43 \pm 0.25
JiGen*	✗	73.97 \pm 0.21	61.94 \pm 0.74	97.40 \pm 1.03	66.90 \pm 0.64	75.05 \pm 0.26
FedAvg*	✓	71.95 \pm 0.06	63.29 \pm 0.06	96.48 \pm 0.18	72.37 \pm 0.06	76.02 \pm 0.08
FedDG*	✓	72.59 \pm 0.30	60.33 \pm 0.07	96.70 \pm 0.20	73.61 \pm 0.17	75.81 \pm 0.16
CSAC	✓	72.46 \pm 0.18	63.59 \pm 0.22	97.80 \pm 0.07	72.67 \pm 0.27	76.63 \pm 0.06

where λ is a semantic calibration hyper-parameter.

Model optimization. We first perform local semantic acquisition by training the local models $\{G^h\}_{h=1}^H$ with Equation (2) for data distribution learning. The trained models are employed to calculate the fused model M for semantic aggregation with Equation (4). We then copy M to each domain for semantic calibration with Equation (11), and fuse the calibrated models again. We repeat the semantic aggregation and calibration alternately to unify semantic learning and alignment in a collaborative way, resulting in a generalizable model \hat{M} for inference on unknown target domains.

Remark. In practice, we assign the parameters of the fused model M to each trained model G^h for simultaneous semantic calibration on each domain h , and fuse them again.

Experiments

We empirically evaluate the proposed CSAC on multiple datasets and provide in-depth ablations and discussions.

Benchmark datasets. We first adopt a simulated digit dataset **Rotated MNIST** (Ghifary et al. 2015) with 6 domains, i.e., *M0*, *M15*, *M30*, *M45*, *M60*, *M75*. We follow (Ghifary et al. 2015; Zhao et al. 2020) and use 100 images per class. Another two popular datasets are employed. One is **PACS** (Li et al. 2017) that covers 7 categories within 4 domain, i.e., *Art*, *Cartoon*, *Sketch*, *Photo*. Another is **VLCS** (Ghifary et al. 2015) that contains 5 classes from 4 domains, i.e., *Pascal*, *LabelMe*, *Caltech*, *Sun*. We split dataset by 0.7/0.3 for training/test, and conduct leave-one-

Table 3: Classification accuracy (%) on PACS dataset. “Sep.”: whether using separated source datasets.

Methods	Sep.	Art	Cartoon	Photo	Sketch	Average
DeepAll*	✗	78.95 \pm 0.48	74.90 \pm 1.82	94.08 \pm 0.55	73.02 \pm 0.80	80.24 \pm 0.50
JiGen	✗	79.42	75.25	96.03	71.35	80.51
MASF	✗	80.29	77.17	94.99	71.69	81.04
DGER	✗	80.70	76.40	96.65	71.77	81.38
Epi-FCR	✗	82.1	77.0	93.9	73.0	81.5
EISNet	✗	81.89	76.44	95.93	74.33	82.15
FedAvg*	✓	77.49 \pm 0.10	77.21 \pm 0.52	93.56 \pm 0.38	81.19 \pm 0.80	82.36 \pm 0.44
FedDG*	✓	78.46 \pm 0.20	75.98 \pm 0.28	93.23 \pm 0.43	80.92 \pm 0.72	82.15 \pm 0.35
CSAC	✓	81.86 \pm 0.08	76.31 \pm 0.09	95.35 \pm 0.30	83.06 \pm 0.12	84.14 \pm 0.09

domain-out experiments by choosing one domain to hold out as the target domain. We then construct a new dataset **Office-Caltech-Home** by choosing the common classes from Office-Caltech (Gong et al. 2012) and Office-Home (Venkateswara et al. 2017) datasets, and merge them to get 7 domains, i.e., Amazon (*Am*), Webcam (*We*), Caltech (*Ca*), Art (*Ar*), Clipart (*Cl*), Product (*Pr*), and Real-World (*Rw*).

Baseline methods. We compare our method CSAC against the representative FL method *FedAvg* (McMahan et al. 2017) and the FL-based generalizable model learning method *FedDG* (Liu et al. 2021) in the proposed separated domain generalization task. We also show the performance of the state-of-the-art DG methods introduced in the related work, i.e., Epi-FCR(Li et al. 2019a), JiGen(Carlucci et al. 2019), MASF(Dou et al. 2019), DGER(Zhao et al. 2020), EISNet(Wang et al. 2020), under the generic DG setting with shared data. We implement *DeepAll* baseline by fusing all the source data and directly using it to train the model.

Implementation details. Following (Ghifary et al. 2015; Zhao et al. 2020), we use standard MNIST CNN architecture with two convolution layers and two fully-connected (FC) layers for Rotated MNIST dataset. We use the pretrained ResNet-18 (He et al. 2016) for PACS, VLCS, and Office-Caltech-Home datasets and also use AlexNet (Krizhevsky, Sutskever, and Hinton 2017) for VLCS, following (Carlucci et al. 2019; Dou et al. 2019; Huang et al. 2020). We extract the convolution layers of the last three blocks of ResNet-18, the last three convolution layers of AlexNet, the last two convolution layers of MNIST CNN, as the layer set for semantic calibration. We implement the methods according to their public code, where the boundary component of FedDG is discarded for fair comparison. We use SGD optimizer with learning rate 0.01 and momentum 0.5 for ResNet-18 and MNIST CNN, and learning rate 0.001 for AlexNet. The training epochs for semantic acquisition are set to 30, collaboration rounds for aggregation and calibration are set to 40, for all the datasets. In each round, the calibration epochs are set to 5 and 10 for Rotated MNIST and other datasets, respectively. The hyper-parameter λ is set to 0.6 for all the experiments. We run the experiments on a device with CPU Xeon Gold 6254 \times 2, and GPU Nvidia RTX 2080 TI \times 4. We report the mean and standard error of the classification accuracy over *three runs* with random seeds for the experiments implemented by us (**marked with ***). And we cite other results of the DG methods from the published papers.

Results. Table 1, 2, and 3 show the results on Rotated

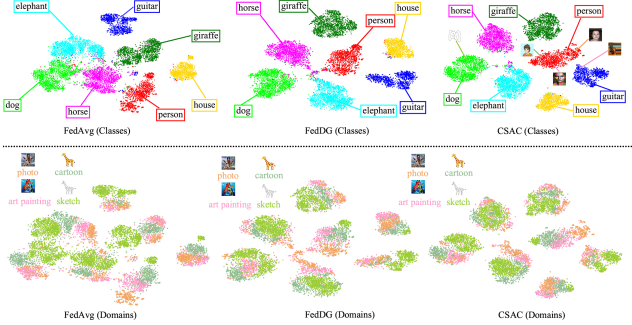
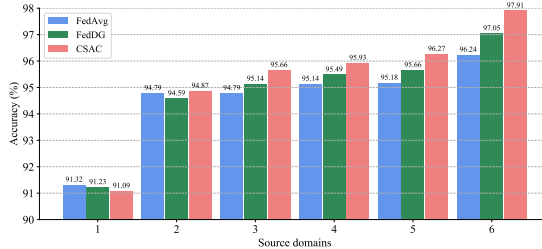


Figure 3: **Left:** Classification accuracy (%) on **Office-Caltech-Home** dataset. We add one source domain each time from the domain set {Am, Cl, Pr, We, Ar, Ca}. Target domain: Rw; **Right:** **T-SNE visualization** of semantic feature distribution on **PACS** dataset. Different colors represent different classes (**above**) and domains (**below**), respectively. Target domain: Photo.

Table 4: Effect of semantic aggregation with **semantic divergence (strategy)** and **L_2 distance (metric)**.

Type	Case	PACS					VLCS				
		Art	Cartoon	Photo	Sketch	Average	Pascal	LabelMe	Caltech	Sun	Average
Strategy	Semantic similarity	79.22 \pm 0.19	72.44 \pm 0.53	93.00 \pm 0.14	74.34 \pm 0.37	79.75 \pm 0.22	70.80 \pm 0.16	62.86 \pm 0.39	96.61 \pm 0.26	69.49 \pm 1.03	74.94 \pm 0.46
	Semantic average	80.25 \pm 0.36	74.54 \pm 0.44	93.74 \pm 0.15	77.88 \pm 0.69	81.85 \pm 0.07	72.44 \pm 0.17	61.20 \pm 0.32	96.54 \pm 0.30	70.83 \pm 0.45	75.25 \pm 0.21
Metric	Cosine distance	80.89 \pm 0.23	73.57 \pm 0.41	94.43 \pm 0.03	76.59 \pm 1.31	81.37 \pm 0.41	72.27 \pm 0.11	62.94 \pm 0.44	97.05 \pm 0.15	71.41 \pm 0.06	75.92 \pm 0.11
	L_1 distance	81.75 \pm 0.51	74.93 \pm 0.09	94.45 \pm 0.28	77.63 \pm 0.42	82.19 \pm 0.27	72.16 \pm 0.16	64.11 \pm 0.28	96.64 \pm 0.13	71.67 \pm 0.21	76.15 \pm 0.04
CSAC		81.86 \pm 0.08	76.31 \pm 0.09	95.35 \pm 0.30	83.06 \pm 0.12	84.14 \pm 0.09	72.46 \pm 0.18	63.59 \pm 0.22	97.80 \pm 0.07	72.67 \pm 0.27	76.63 \pm 0.06

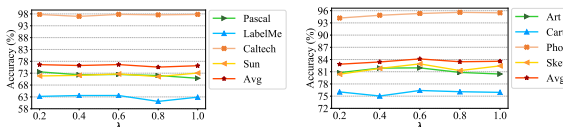


Figure 4: **Sensitivity analysis** of semantic calibration hyper-parameter λ on VLCS (**left**) and PACS (**right**) datasets.

MNIST, VLCS, and PACS datasets, respectively. We observe that CSAC performs the best on about more than half of the separated domain generalization tasks by comparing with FedAvg and FedDG, and also achieves the highest average classification accuracy on all the datasets. We then notice that CSAC can even exhibit comparable or even better model generalization performance than the DG methods with shared data, especially with larger networks (ResNet-18) and larger datasets (PACS), which indicates that the generalizable model can be effectively trained with privacy protection. Figure 3 (left) illustrates the results with more source domains, where CSAC shows significant generalization improvement. We attribute it to the effectiveness of collaborative semantic aggregation and calibration of CSAC, and more source domains facilitate the semantic level alignment and domain invariance learning during this process.

In-Depth Ablation Studies

Semantic aggregation. Table 4 reports in-depth ablation results for semantic aggregation. By replacing the strategy with semantic similarity (larger weights for the models that are closer to the average distribution) and average (equal weights), we find that it is important to pay more attention to

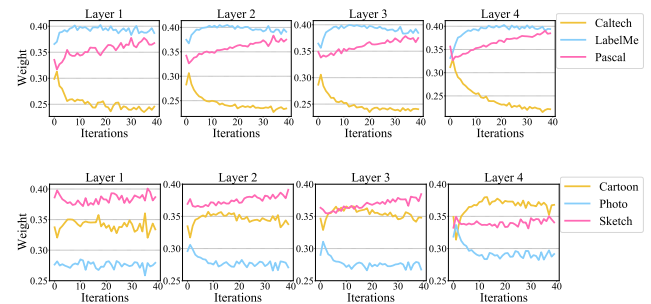


Figure 5: **Semantic divergence based weight** for the last layer of the four blocks of ResNet-18 of each trained model (marked with the corresponding source) during semantic aggregation on VLCS (**above**) and PACS (**below**) datasets.

the domain with the semantic distribution far from the others for fairly absorbing all the domain knowledge, facilitating valid domain invariance learning. The experiments with other metrics show the effectiveness of the used L_2 distance.

Semantic calibration. Table 5 reports in-depth ablation results for semantic calibration. We compare the results without alignment and using the same-layer alignment and find that it is necessary to consider cross-layer semantic relationships for addressing the semantic dislocation problem. By conducting the attention ablations, we demonstrate the attention mechanism with both position and channel interdependency consideration is important for precise semantic level alignment. The label smoothing is showed useful for a final generalizable model learning, which is may because it leads to more smooth models for stable model fusion. Cross-

Table 5: Effect of semantic calibration with cross-layer alignment (strategy) and MMD discrepancy (metric).

Type	Case	PACS					VLCS				
		Art	Cartoon	Photo	Sketch	Average	Pascal	LabelMe	Caltech	Sun	Average
Strategy	Without alignment	80.34 \pm 0.24	76.07 \pm 0.14	95.45 \pm 0.49	81.11 \pm 0.12	83.24 \pm 0.15	70.11 \pm 1.21	65.73 \pm 2.31	97.03 \pm 0.15	71.39 \pm 0.16	76.06 \pm 0.75
	Same-layer alignment	80.49 \pm 0.23	74.19 \pm 0.11	94.85 \pm 0.55	80.34 \pm 0.44	82.46 \pm 0.17	73.51 \pm 0.21	62.26 \pm 0.14	97.38 \pm 0.08	71.38 \pm 0.14	76.14 \pm 0.12
	Without attention (position)	79.57 \pm 0.44	73.57 \pm 0.61	94.46 \pm 0.12	79.66 \pm 0.47	81.82 \pm 0.16	72.57 \pm 0.12	63.85 \pm 0.78	96.09 \pm 0.26	69.16 \pm 0.21	75.42 \pm 0.31
	Without attention (channel)	79.80 \pm 0.58	73.77 \pm 0.03	94.43 \pm 0.09	79.32 \pm 0.19	81.83 \pm 0.14	72.40 \pm 0.52	63.54 \pm 0.52	95.92 \pm 0.30	69.24 \pm 0.12	75.27 \pm 0.20
	Without attention	80.35 \pm 0.87	76.27 \pm 0.11	93.59 \pm 0.24	77.88 \pm 1.53	82.02 \pm 0.58	71.63 \pm 0.06	64.48 \pm 2.46	96.27 \pm 0.40	67.67 \pm 1.03	75.01 \pm 0.44
	Without label smoothing	81.79 \pm 0.04	76.19 \pm 0.15	95.31 \pm 0.24	83.03 \pm 0.09	84.08 \pm 0.11	72.39 \pm 0.09	63.50 \pm 0.16	97.72 \pm 0.07	72.56 \pm 0.12	76.54 \pm 0.01
Metric	Mean Square Error (MSE)	77.08 \pm 0.28	71.05 \pm 1.26	94.61 \pm 0.14	75.99 \pm 0.33	79.68 \pm 0.49	72.10 \pm 0.79	62.17 \pm 0.19	96.47 \pm 0.35	71.09 \pm 0.14	75.46 \pm 0.26
	CSAC	81.86 \pm 0.08	76.31 \pm 0.09	95.35 \pm 0.30	83.06 \pm 0.12	84.14 \pm 0.09	72.46 \pm 0.18	63.59 \pm 0.22	97.80 \pm 0.07	72.67 \pm 0.27	76.63 \pm 0.06

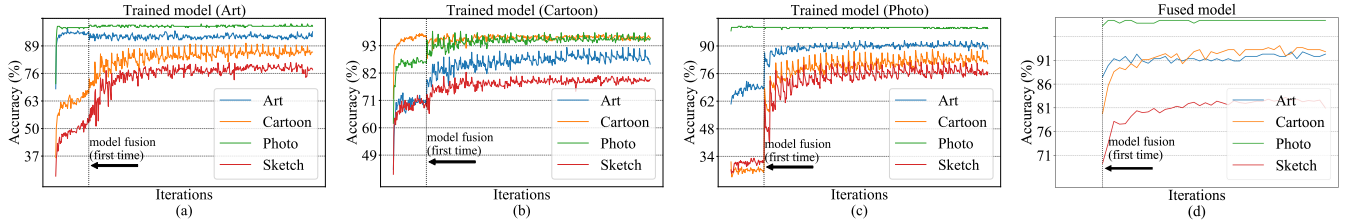


Figure 6: Accuracy (on each dataset) of the trained models, i.e., (a-c), and fused model, i.e., (d), during the whole training process, i.e., semantic acquisition and the repeat of semantic aggregation and calibration. Dataset: PACS; Target domain: Sketch.

Table 6: Run time (hours) on PACS and VLCS datasets.

Methods	PACS					VLCS				
	Photo	Art	Cartoon	Sketch	Average	Pascal	LabelMe	Caltech	Sun	Average
FedAvg	3.85	3.95	4.03	4.32	4.04	3.03	3.10	3.08	3.11	3.08
FedDG	11.65	11.84	11.92	12.01	11.86	10.81	10.43	10.50	10.19	10.48
CSAC	4.81	4.81	4.48	4.34	4.61	3.61	3.61	3.57	3.59	3.60

entropy displays its importance for catastrophic forgetting. The MMD metric is more effective for semantic alignment than the MSE, which may also be the reason that MMD is widely adopted in alignment-based domain adaptation.

Sensitivity analysis. Figure 4 shows that CSAC is generally robust to a proper weight for the semantic calibration, i.e., hyper-parameter λ , showing that CSAC is practical without time-consuming hyper-parameter fine-tuning.

Run Time

We report the run time of the methods (implemented locally) in Table 6. FedDG is computationally inefficient by using about three times the run time of FedAvg and CSAC, which is may because of the time-consuming process of the distribution bank building. Besides, FedDG transmits the bank to all the domains, which needs high communication costs and increases risks of privacy leakage (although we can not verify it with experiments), as we discussed in related work.

Why Does CSAC Work?

We observe that the weight curves have the same trend in Figure 5, i.e., the four extracted layers of each model have the same semantic divergence to others, which indirectly verifies our hypothesis that parameters are related to the training data (we will discuss it in detail in Appendix). The model with divergent semantics is given large weight layer-by-layer for adequate semantic learning, facilitating the following semantic calibration, as testified in ablation studies.

Figure 3 (right) shows comparisons on the learned semantic feature distributions. CSAC obtains more discriminative

and domain-agnostic information and generates class clear and domain compact semantic features. We attribute it to the effectiveness of collaborative semantic aggregation and calibration for domain invariance learning with separated data.

We then present insights on the proposed CSAC via showing the accuracy curves of the models on each dataset during training in Figure 6 (note that the target dataset is only used for testing the accuracy). During semantic acquisition, each trained model is assigned to each separated domain for data distribution learning, and its accuracy on the learned dataset improves rapidly (see the parts before model fusion of sub-figure (a-c)). The accuracy of the trained models assigned to Art, Cartoon, and Photo domain, on the target dataset, i.e., Sketch (red curve at dotted line), is 52.74%, 68.47%, 32.02%, respectively, before model fusion. Then, the trained models are fused for semantic aggregation, each domain knowledge is fully gathered. The parameters of the fused model are then assigned to each trained model again with each source data for semantic calibration. We unify semantic learning and alignment by repeating semantic aggregation and calibration alternately, the domain invariance from the separated domains is indirectly captured, making the accuracy of the fused model (subfigure (d)) has been improved gradually on all the datasets. By comparing the results before model fusion, the accuracy on the target dataset finally reaches an improvement of more than 29%, 13%, and 50%.

Conclusions

Training a generalizable model is a vital issue for the deep learning community. However, common practices of domain generalization rely on shared multi-source data, which may violate privacy policies in real-world applications. This paper investigates a privacy-preserving task named separated domain generalization, and gives a novel solution to this

challenging task with collaborative semantic aggregation and calibration, which unifies multi-source semantic learning and alignment in a collaborative way. The limitations of this work may be the homogeneous architecture and space of the used deep models and source data, respectively, and future work may extend them to more complex scenarios.

References

- Bahdanau, D.; Cho, K.; and Bengio, Y. 2015. Neural Machine Translation by Jointly Learning to Align and Translate. In *ICLR*.
- Balaji, Y.; Sankaranarayanan, S.; and Chellappa, R. 2018. Metareg: Towards domain generalization using meta-regularization. In *NeurIPS*, 998–1008.
- Blanchard, G.; Lee, G.; and Scott, C. 2011. Generalizing from several related classification tasks to a new unlabeled sample. *NeurIPS*, 24: 2178–2186.
- Carlucci, F. M.; D’Innocente, A.; Bucci, S.; Caputo, B.; and Tommasi, T. 2019. Domain Generalization by Solving Jigsaw Puzzles. *CVPR*, 2224–2233.
- Chattpadhyay, P.; Balaji, Y.; and Hoffman, J. 2020. Learning to balance specificity and invariance for in and out of domain generalization. In *ECCV*, 301–318. Springer.
- Dou, Q.; de Castro, D. C.; Kamnitsas, K.; and Glocker, B. 2019. Domain Generalization via Model-Agnostic Learning of Semantic Features. In *NeurIPS*.
- Fu, J.; Liu, J.; Tian, H.; Li, Y.; Bao, Y.; Fang, Z.; and Lu, H. 2019. Dual Attention Network for Scene Segmentation. In *CVPR*, 3146–3154.
- Ganin, Y.; Ustinova, E.; Ajakan, H.; Germain, P.; Larochelle, H.; Laviolette, F.; Marchand, M.; and Lempitsky, V. 2016. Domain-adversarial training of neural networks. *JMLR*, 17(1): 2096–2030.
- Ghifary, M.; Bastiaan Kleijn, W.; Zhang, M.; and Balduzzi, D. 2015. Domain generalization for object recognition with multi-task autoencoders. In *ICCV*, 2551–2559.
- Ghosh, A.; Chung, J.; Yin, D.; and Ramchandran, K. 2020. An efficient framework for clustered federated learning. *NeurIPS*.
- Gong, B.; Shi, Y.; Sha, F.; and Grauman, K. 2012. Geodesic flow kernel for unsupervised domain adaptation. In *CVPR*, 2066–2073. IEEE.
- Goodfellow, I. J.; Mirza, M.; Xiao, D.; Courville, A.; and Bengio, Y. 2013. An empirical investigation of catastrophic forgetting in gradient-based neural networks. *arXiv*.
- Gretton, A.; Borgwardt, K. M.; Rasch, M. J.; Schölkopf, B.; and Smola, A. 2012. A kernel two-sample test. *JMLR*, 13(1): 723–773.
- He, K.; Zhang, X.; Ren, S.; and Sun, J. 2016. Deep residual learning for image recognition. In *CVPR*, 770–778.
- Huang, Z.; Wang, H.; Xing, E. P.; and Huang, D. 2020. Self-challenging Improves Cross-Domain Generalization. In *ECCV*, 124–140.
- Krizhevsky, A.; Sutskever, I.; and Hinton, G. E. 2017. ImageNet classification with deep convolutional neural networks. *Commun. ACM*, 60(6): 84–90.
- Kundu, J. N.; Venkat, N.; Babu, R. V.; et al. 2020. Universal source-free domain adaptation. In *CVPR*, 4544–4553.
- Li, D.; Yang, Y.; Song, Y.-Z.; and Hospedales, T. 2018a. Learning to generalize: Meta-learning for domain generalization. In *AAAI*, volume 32.
- Li, D.; Yang, Y.; Song, Y.-Z.; and Hospedales, T. M. 2017. Deeper, broader and artier domain generalization. In *ICCV*, 5542–5550.
- Li, D.; Zhang, J.; Yang, Y.; Liu, C.; Song, Y.-Z.; and Hospedales, T. M. 2019a. Episodic Training for Domain Generalization. *ICCV*, 1446–1455.
- Li, H.; Jialin Pan, S.; Wang, S.; and Kot, A. C. 2018b. Domain generalization with adversarial feature learning. In *CVPR*, 5400–5409.
- Li, H.; Wang, Y.; Wan, R.; Wang, S.; Li, T.; and Kot, A. C. 2020a. Domain Generalization for Medical Imaging Classification with Linear-Dependency Regularization. In *NeurIPS*.
- Li, R.; Jiao, Q.; Cao, W.; Wong, H.-S.; and Wu, S. 2020b. Model adaptation: Unsupervised domain adaptation without source data. In *CVPR*, 9641–9650.
- Li, Y.; Gong, M.; Tian, X.; Liu, T.; and Tao, D. 2018c. Domain generalization via conditional invariant representations. In *AAAI*, volume 32.
- Li, Y.; Tian, X.; Gong, M.; Liu, Y.; Liu, T.; Zhang, K.; and Tao, D. 2018d. Deep domain generalization via conditional invariant adversarial networks. In *ECCV*, 624–639.
- Li, Y.; Yang, Y.; Zhou, W.; and Hospedales, T. 2019b. Feature-critic networks for heterogeneous domain generalization. In *ICML*, 3915–3924. PMLR.
- Liang, J.; Hu, D.; and Feng, J. 2020. Do we really need to access the source data? source hypothesis transfer for unsupervised domain adaptation. In *ICML*, 6028–6039. PMLR.
- Lin, T.; Kong, L.; Stich, S. U.; and Jaggi, M. 2020. Ensemble distillation for robust model fusion in federated learning. *NeurIPS*.
- Liu, Q.; Chen, C.; Qin, J.; Dou, Q.; and Heng, P.-A. 2021. FedDG: Federated Domain Generalization on Medical Image Segmentation via Episodic Learning in Continuous Frequency Space. *arXiv*.
- Long, M.; Cao, Y.; Wang, J.; and Jordan, M. 2015. Learning transferable features with deep adaptation networks. In *ICML*, 97–105. PMLR.
- Long, M.; Zhu, H.; Wang, J.; and Jordan, M. I. 2016. Unsupervised Domain Adaptation with Residual Transfer Networks. In *NeurIPS*.
- Long, M.; Zhu, H.; Wang, J.; and Jordan, M. I. 2017. Deep transfer learning with joint adaptation networks. In *ICML*, 2208–2217. PMLR.
- Matsuura, T.; and Harada, T. 2020. Domain Generalization Using a Mixture of Multiple Latent Domains. In *AAAI*.
- McCloskey, M.; and Cohen, N. J. 1989. Catastrophic interference in connectionist networks: The sequential learning problem. In *Psychology of learning and motivation*, volume 24, 109–165. Elsevier.

- McMahan, B.; Moore, E.; Ramage, D.; Hampson, S.; and y Arcas, B. A. 2017. Communication-efficient learning of deep networks from decentralized data. In *AISTATS*, 1273–1282. PMLR.
- Müller, R.; Kornblith, S.; and Hinton, G. E. 2019. When Does Label Smoothing Help? In *NeurIPS*.
- Peng, X.; Huang, Z.; Zhu, Y.; and Saenko, K. 2020. Federated adversarial domain adaptation. *ICLR*.
- Piratla, V.; Netrapalli, P.; and Sarawagi, S. 2020. Efficient Domain Generalization via Common-Specific Low-Rank Decomposition. In *ICML*.
- Qiao, F.; Zhao, L.; and Peng, X. 2020. Learning to learn single domain generalization. In *CVPR*, 12556–12565.
- Quionero-Candela, J.; Sugiyama, M.; Schwaighofer, A.; and Lawrence, N. D. 2009. *Dataset shift in machine learning*. The MIT Press.
- Seo, S.; Suh, Y.; Kim, D.; Han, J.; and Han, B. 2020. Learning to Optimize Domain Specific Normalization for Domain Generalization. In *ECCV*.
- Shankar, S.; Piratla, V.; Chakrabarti, S.; Chaudhuri, S.; Jyothi, P.; and Sarawagi, S. 2018. Generalizing Across Domains via Cross-Gradient Training. In *ICLR*.
- Venkateswara, H.; Eusebio, J.; Chakraborty, S.; and Panchanathan, S. 2017. Deep hashing network for unsupervised domain adaptation. In *CVPR*, 5018–5027.
- Volpi, R.; Namkoong, H.; Sener, O.; Duchi, J. C.; Murino, V.; and Savarese, S. 2018. Generalizing to unseen domains via adversarial data augmentation. In *NeurIPS*, 5334–5344.
- Wang, F.; Jiang, M.; Qian, C.; Yang, S.; Li, C.; Zhang, H.; Wang, X.; and Tang, X. 2017. Residual Attention Network for Image Classification. In *CVPR*, 3156–3164.
- Wang, S.; Yu, L.; Li, C.; Fu, C.-W.; and Heng, P. 2020. Learning from Extrinsic and Intrinsic Supervisions for Domain Generalization. In *ECCV*.
- Wang, Y.; Su, H.; Zhang, B.; and Hu, X. 2018. Interpret Neural Networks by Identifying Critical Data Routing Paths. *CVPR*, 8906–8914.
- Yang, Q.; Liu, Y.; Chen, T.; and Tong, Y. 2019. Federated machine learning: Concept and applications. *TIST*, 10(2):1–19.
- Yoon, T.; Shin, S.; Hwang, S. J.; and Yang, E. 2021. FED-MIX: Approximation of Mixup under Mean Augmented Federated Learning. In *ICLR*.
- Zhang, H.; Goodfellow, I.; Metaxas, D.; and Odena, A. 2019a. Self-Attention Generative Adversarial Networks. In *ICML*, 7354–7363. PMLR.
- Zhang, Q.; Yang, Y.; Wu, Y.; and Zhu, S. 2019b. Interpreting CNNs via Decision Trees. *CVPR*, 6254–6263.
- Zhao, S.; Gong, M.; Liu, T.; Fu, H.; and Tao, D. 2020. Domain Generalization via Entropy Regularization. In *NeurIPS*.
- Zhou, K.; Yang, Y.; Hospedales, T.; and Xiang, T. 2020a. Deep domain-adversarial image generation for domain generalisation. In *AAAI*, volume 34, 13025–13032.
- Zhou, K.; Yang, Y.; Hospedales, T.; and Xiang, T. 2020b. Learning to generate novel domains for domain generalization. In *ECCV*, 561–578.
- Zhou, K.; Yang, Y.; Qiao, Y.; and Xiang, T. 2021. Domain Generalization with Mixstyle. In *ICLR*.